



**CHALMERS**  
UNIVERSITY OF TECHNOLOGY

## Halo effects in the low-energy scattering of $^{15}\text{C}$ with heavy targets

Downloaded from: <https://research.chalmers.se>, 2026-04-03 05:51 UTC

Citation for the original published paper (version of record):

Ovejas, J., Knyazev, A., Martel, I. et al (2020). Halo effects in the low-energy scattering of  $^{15}\text{C}$  with heavy targets. *Acta Physica Polonica, Series B.*, 51(3): 731-736.  
<http://dx.doi.org/10.5506/APhysPolB.51.731>

N.B. When citing this work, cite the original published paper.

## HALO EFFECTS IN THE LOW-ENERGY SCATTERING OF $^{15}\text{C}$ WITH HEAVY TARGETS\*

J.D. OVEJAS<sup>a</sup>, A. KNYAZEV<sup>b</sup>, I. MARTEL<sup>c,d</sup>, O. TENGBLAD<sup>a</sup>  
 M.J.G. BORGE<sup>a</sup>, J. CEDERKÄLL<sup>b</sup>, N. KEELEY<sup>e</sup>, K. RUSEK<sup>f</sup>  
 C. GARCÍA-RAMOS<sup>d</sup>, L.A. ACOSTA<sup>g</sup>, A.A. AROKIARAJ<sup>h</sup>, M. BABO<sup>h</sup>  
 T. CAP<sup>e</sup>, N. CEYLAN<sup>d</sup>, G. DE ANGELIS<sup>i</sup>, A. DI PIETRO<sup>j</sup>  
 J.P. FERNÁNDEZ<sup>j</sup>, P. FIGUERA<sup>j</sup>, L. FRAILE<sup>k</sup>, H. FYNBO<sup>l</sup>, D. GALAVIZ<sup>m</sup>  
 J.H. JENSEN<sup>l</sup>, B. JONSON<sup>n</sup>, R. KOTAK<sup>o</sup>, T. KURTUKIAN<sup>p</sup>  
 M. MADURGA<sup>q</sup>, G. MARQUÍNEZ-DURÁN<sup>d</sup>, M. MUNCH<sup>l</sup>, A.K. ORDUZ<sup>r</sup>  
 R. HONÓRIO<sup>m</sup>, A. PAKOU<sup>s</sup>, T. PÉREZ<sup>d</sup>, L. PERALTA<sup>m</sup>, A. PEREA<sup>a</sup>  
 R. RAABE<sup>h</sup>, M. RENAUD<sup>h</sup>, K. RIISAGER<sup>l</sup>, A.M. SÁNCHEZ-BENÍTEZ<sup>d</sup>  
 J. SÁNCHEZ-SEGOVIA<sup>d</sup>, O. SGOUROS<sup>s</sup>, V. SOUKERAS<sup>s</sup>, P. TEUBIG<sup>m</sup>  
 S. VIÑALS<sup>a</sup>, M. WOLIŃSKA-CIHOCKA<sup>f</sup>, R. WOLSKI<sup>t</sup>, J. YANG<sup>h</sup>

<sup>a</sup>Instituto de Estructura de la Materia — CSIC, Madrid

<sup>b</sup>Lund University, Sweden

<sup>c</sup>University of Liverpool, UK

<sup>d</sup>University of Huelva, Spain

<sup>e</sup>National Centre for Nuclear Research, Poland

<sup>f</sup>Heavy Ion Laboratory, University of Warsaw, Poland

<sup>g</sup>Instituto de Física UNAM, Mexico

<sup>h</sup>KU Leuven, Belgium

<sup>i</sup>INFN Laboratori Nazionali di Legnaro, Italy

<sup>j</sup>INFN Laboratori Nazionali del Sud, Italy

<sup>k</sup>Universidad Complutense de Madrid, Spain

<sup>l</sup>Aarhus University, Denmark

<sup>m</sup>LIP Lisbon, Portugal

<sup>n</sup>Chalmers University of Technology, Sweden

<sup>o</sup>Queen's University Belfast, UK

<sup>p</sup>Centre d'Etudes Nucléaires de Bordeaux Gradignan, France

<sup>q</sup>Texas A&M University, USA

<sup>r</sup>GANIL, France

<sup>s</sup>Department of Physics and HINP, Greece

<sup>t</sup>Institute of Nuclear Physics Polish Academy of Sciences, Poland

*(Received January 15, 2020)*

---

\* Presented at the XXXVI Mazurian Lakes Conference on Physics, Piaski, Poland, September 1–7, 2019.

The neutron-rich carbon isotope  $^{15}\text{C}$  was postulated to be a halo nucleus ( $S_n = 1215$  keV,  $S_{2n} = 9395$  keV) according to different high-energy experiments. If so, it would be the only halo nucleus exhibiting a “pure” s-wave structure of the ground state. At low collision energies, the effect of this halo structure should manifest as a strong absorption pattern in the angular distribution of the elastic cross section, with a total suppression of the nuclear rainbow due to the large neutron transfer and breakup probabilities, enhanced by the halo configuration. The IS619 experiment, carried out at the HIE-ISOLDE facility at CERN (Switzerland), is the first dynamical study of this nucleus at energies around the Coulomb barrier. It aims to probe the halo structure via the measurement of the elastic cross section on a high- $Z$   $^{208}\text{Pb}$  target. Preliminary results of the elastic cross section are discussed and compared to Optical Model calculations.

DOI:10.5506/APhysPolB.51.731

## 1. Introduction

In the light region of the nuclear chart, close to the driplines, systems such as  $^6\text{He}$ ,  $^{11}\text{Li}$  or  $^{11}\text{Be}$  are found to have an extended neutron distribution; the so-called halo structure. This configuration is understood as a threshold effect, where the reduced binding energy of the last valence nucleons allows them for tunnelling out of the Coulomb barrier. This causes an exceptionally large matter density distribution and a very diffuse nuclear surface [1]. The halo structure leads to characteristic features in nuclear reactions and thus can be studied via scattering. At high-energies (above 100 MeV/ $u$ ), a neutron halo will produce a narrow longitudinal momentum distribution of the breakup fragments and a large value of the interaction cross section [2, 3]. However, at low collision energies, near the Coulomb barrier (around 5 MeV/ $u$ ), the dynamics of the system is dominated by collective degrees of freedom, and is characterized by the coupling between the elastic, transfer and breakup channels, and the effects of the continuum. Here, the halo leaves a strong absorption pattern in the elastic cross sections and the nuclear rainbow completely disappears [4–7].

The last valence neutron in the  $^{15}\text{C}$  isotope has a predominantly  $2s_{1/2}$  wave function [8], which favours presence of a halo structure despite a relatively large binding energy  $S_n = 1218.1(8)$  keV [9]. Its total interaction cross section is 30% larger than those of the neighbouring isotopes and the transverse-momentum distribution following breakup exhibits a remarkably narrow width of 67(3) MeV/ $c$  [10]. At low energies, coupled-channels calculations predict a competition between neutron transfer and breakup [12], however, no experimental studies have been possible yet [11]. Making use of the recently inaugurated HIE-ISOLDE facility, we have investigated the scattering of  $^{15}\text{C}$  on a  $^{208}\text{Pb}$  target at a beam energy of 65 MeV to clarify its behaviour.

## 2. Experimental setup

The IS619 experiment was carried out in August 2017 using the Scattering Experiment Chamber at the XT03 beamline of the HIE-ISOLDE facility at CERN (Switzerland). The  $^{15}\text{C}^{5+}$  beam was produced by spallation from the impact of the PS Booster 1.4 GeV proton pulses on a CaO primary target connected to a hot-cathode plasma source. The isotope of interest was extracted, purified, mass-separated and injected into the High Intensity and Energy superconducting linac, where it was post-accelerated up to 4.37 MeV/ $u$  (barrier energy for the system projectile+target), and directed onto  $^{208}\text{Pb}$  secondary targets of 2.1 and 1.2 mg/cm<sup>2</sup> thicknesses.

The measurement of fragments produced in the reaction was performed with GLORIA [13], consisting of 6 silicon telescopes, each made of two 16×16 strips DSSDs; a 40  $\mu\text{m}$  thick  $\Delta E$  in front of a 1 mm thick  $E$  (see a scheme in Fig. 1). The detectors surrounded the reaction target covering the scattering angles from 15° to 165° in the laboratory frame, with a total geometric efficiency of 25% of  $4\pi$ , and an angular resolution between 2 and 3°.

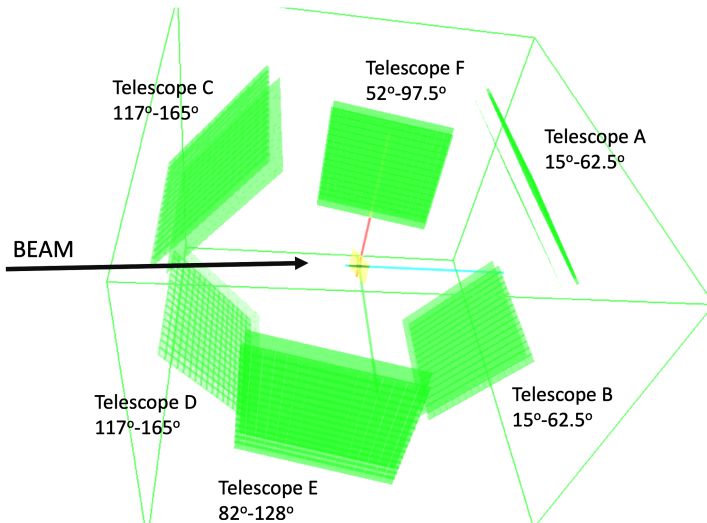


Fig. 1. 3D scheme of the GLORIA detectors arrangement with the reaction target in the center.

Other nuclei with the same  $A/Q$  ratio such as  $^{12}\text{C}^{4+}$ ,  $^{15}\text{N}^{5+}$  and  $^{18}\text{O}^{6+}$  were present in the beam as residual gases coming from the EBIS, however, after a 75  $\mu\text{g}/\text{cm}^2$  carbon stripping foil, all of them were totally removed except for nitrogen, remaining in a fraction  $^{15}\text{C}/^{15}\text{N} \simeq 0.03$ . The  $^{15}\text{C}$  intensity, on the secondary Pb target, was close to  $10^3$  pps. The scattered nitrogen

can be well-separated from carbon in the 2D plot. As the  $^{15}\text{N}$  energy is well below its Coulomb barrier for lead, the elastic differential cross section will follow a classical Rutherford distribution.

### 3. Data analysis and experimental results

The  $\Delta E$ - $E$  detectors in a telescope configuration enable fragment identification as it is demonstrated in Fig. 2. A polygon cut can be imposed in the corresponding zone of the elastically scattered  $^{15}\text{N}$  and  $^{15}\text{C}$  events, which are subsequently integrated pixel by pixel. The scattering angles associated to the center of each pixel, as well as their solid angles, are improved by a  $\chi^2$  fit of the angular distribution of the  $^{15}\text{N}$  ions, assuming a pure Rutherford scattering distribution.

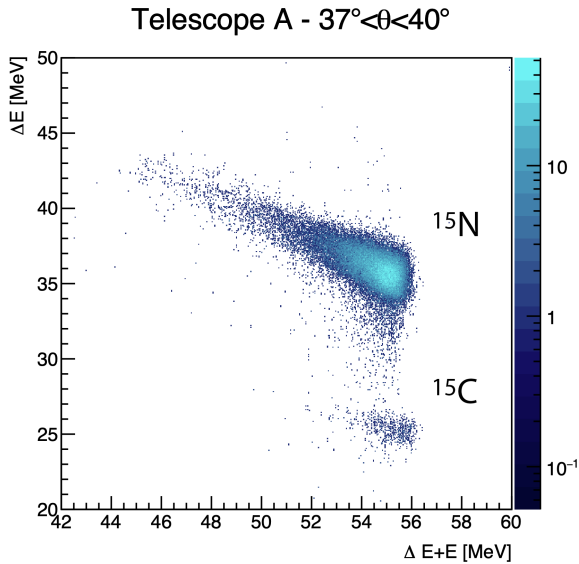


Fig. 2. 2D plot from the pixels comprised in the angular interval  $37$ – $40^\circ$  of telescope A (see Fig. 1). The data shown were taken with a  $2.1 \text{ mg/cm}^2$  target. Charge-sharing events have been removed and a geometric energy correction was applied to the  $\Delta E$  axis.

The elastic cross section of  $^{15}\text{C}$  normalized to Rutherford is obtained from the ratio between  $^{15}\text{C}$  and  $^{15}\text{N}$  yields after normalization to unity at the most forward angles. All the points coming from the different pixels in telescopes A and B are averaged considering their respective errors by calculating the weighted arithmetic mean. The result is shown in Fig. 3.

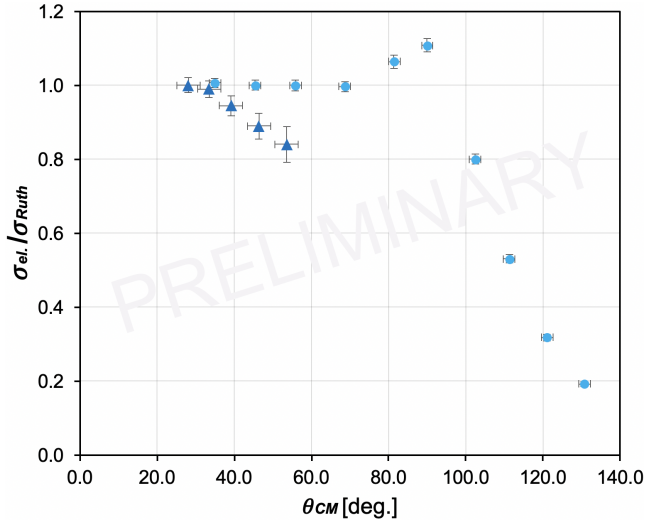


Fig. 3. (Colour on-line) Measured angular distribution of the elastic scattering of  $^{15}\text{C}$  on  $^{208}\text{Pb}$  at  $E_{\text{LAB}} = 65$  MeV denoted with dark blue triangles. Elastic scattering of the non-halo  $^{12}\text{C}$  with the same target and energy is shown for comparison using light blue squares (data from [14]).

The angular distribution of the obtained cross section shows a strong absorption pattern and the nuclear interference suppression in the elastic channel. In the framework of the Optical Model, potential parameters are adjusted in order to reproduce the general trend of the experimental data. A remarkable diffuseness of the imaginary potential is found, which has to be set to  $a_{i0} = 1.56$  fm, more than 4 times the one used to reproduce the  $^{12}\text{C}$  scattering [14]. This suggests an extraordinarily large neutron distribution. The values used for both real and imaginary radii  $r_{r0}$  and  $r_{i0}$  are 1.256 fm and the well depths are 32.9 MeV for the real  $V_0$  part and 22.1 MeV for the  $W_0$  imaginary one.

I. Martel and O. Tengblad, as spokespersons, are grateful to the IS619 Collaboration and to the HIE-ISOLDE team for delivering the radioactive beam. J.D. Ovejas is grateful to AEI/FEDER/EU for the Ph.D. fellowship BES2016-077059. Work partially supported by the Spanish research grants FPA2015-64969-P, FPA2017-87568-P (both AEI/FEDER/EU), PGC 2018-095640-B-I00 and ENSAR2 from EU H2020 under contract number 654002.

## REFERENCES

- [1] I. Tanihata *et al.*, *Phys. Rev. Lett.* **55**, 2676 (1985).
- [2] T. Kobayashi *et al.*, *Phys. Rev. Lett.* **60**, 2599 (1988).
- [3] N.A. Orr *et al.*, *Phys. Rev. Lett.* **69**, 2050 (1992).
- [4] M. Cubero *et al.*, *Phys. Rev. Lett.* **109**, 262701 (2012).
- [5] V. Pesudo *et al.*, *Phys. Rev. Lett.* **118**, 152502 (2017).
- [6] J.P. Fernández-García *et al.*, *Phys. Rev. C* **92**, 044608 (2015).
- [7] G. Marquínez-Durán *et al.*, *Phys. Rev. C* **94**, 064618 (2016).
- [8] J.R. Terry *et al.*, *Phys. Rev. C* **69**, 054306 (2004).
- [9] G. Audi, A.H. Wapstra, *Nucl. Phys. A* **565**, 66 (1993).
- [10] A. Ozawa, *Nucl. Phys. A* **738**, 38 (2004).
- [11] N. Keeley, N. Alamanos, *Phys. Rev. C* **75**, 054610 (2007).
- [12] N. Keeley, K.W. Kemper, K. Rusek, *Eur. Phys. J. A* **50**, 145 (2014).
- [13] G. Marquínez-Durán *et al.*, *Nucl. Instrum. Methods Phys. Res. A* **755**, 69 (2014).
- [14] S. Santra *et al.*, *Phys. Rev. C* **64**, 024602 (2001).